

Reliable prediction of giant magnetoresistance characteristics

M. Ye. Zhuravlev,^{1,*} W. Schepper,¹ S. Heitmann,¹ H. Vinzelberg,² P. Zahn,³ I. Mertig,⁴ H. O. Lutz,¹ A. V. Vedyayev,^{5,†}
G. Reiss,¹ and A. Hütten¹

¹Fakultät für Physik, Universität Bielefeld, Universität Strasse 25, D-33501 Bielefeld, Germany

²IFW Dresden, Helmholtzstrasse 20, D-01069 Dresden, Germany

³Institut für Theoretische Physik, Technische Universität Dresden, Zellerscher Weg 17, D-01062 Dresden, Germany

⁴Martin-Luther-Universität Halle-Wittenberg, Von-Seckendorff-Platz 1, D-06099 Halle, Germany

⁵CEA/Département de Recherche Fondamentale sur la Matière Condensée, SP2M/NM, 38054 Grenoble, France

(Received 25 January 2002; published 1 April 2002)

We present a combined theoretical approach to the giant magnetoresistance (GMR) effect in magnetic multilayers which is able to provide good agreement with experimentally obtained GMR characteristics. This approach is based on a quantum statistical treatment, using as input the numerically determined orientation of the magnetic moments in the magnetic layers. It may be applied to determine spin-dependent transport properties, and to predict GMR characteristics for specific applications.

DOI: 10.1103/PhysRevB.65.144428

PACS number(s): 75.70.Pa, 72.25.Ba, 73.21.Ac, 75.30.Et

Antiferromagnetic coupling in ferromagnetic/paramagnetic-sandwich layers results in a magnetoresistance of unusually high magnitude. This so-called giant magnetoresistance (GMR) is one of the transport phenomena in solid state physics which has stimulated widespread research activities over the past decade due to its fundamental interest as well as its application potential (e.g., see Ref. 1). *Ab initio* calculations (e.g., Ref. 2) based on realistic band structures, as well as a variety of other models^{3–6} have been developed to provide a physical understanding of the GMR effect. Obviously, a reliable knowledge of the predictive power of such calculations would be highly desirable. We have, therefore, performed a joined experimental and theoretical study to explore the ability of a quantum statistical treatment to predict the GMR of multilayered systems. As prototypes we chose magnetron sputtered “combination multilayers” (CML’s) of type

$$\text{Py}_{1.8 \text{ nm}} // \{ [\text{Cu}_{1.8 \text{ nm}} / \text{Py}_{1.6 \text{ nm}}]_N / [\text{Cu}_{0.9 \text{ nm}} / \text{Py}_{1.6 \text{ nm}}]_N \} Y$$

(with Py = Ni₈₁Fe₁₉) because of the following reasons. First, it has been shown experimentally^{7,8} that the GMR of these CML’s are free of hysteresis and depend very distinctly on the value of N . Whereas CML’s with $N=1$ are basically averaging over the two underlying base systems $\{\text{Cu}_{0.9 \text{ nm}} / \text{Py}_{1.6 \text{ nm}}\}_N$ at the first and $\{\text{Cu}_{1.8 \text{ nm}} / \text{Py}_{1.6 \text{ nm}}\}_N$ at the second antiferromagnetic coupling maximum (AFCM),

the CML with $N \geq 2$ results in a superposition of the two base systems weighted by the fraction of their double layer conductance. Secondly, numerical calculations⁹ have been performed to explore the magnetic reversal process of each individual magnetic layer of these CML’s on the basis of an extended Stoner-Wohlfarth model in the single domain limit. Thus, the field dependence of the angles between adjacent magnetization vectors is known and can directly be used as input for the quantum statistical calculation of the GMR versus field characteristics.

Our model is based on the quantum statistical theory which was originally developed to describe the GMR in trilayered systems¹⁰ and treats the transport properties within the Kubo linear response formalism. It is assumed that the s electrons provide the main contribution to the current as a consequence of their lower effective mass compared to that of the d electrons. A free-electron model is used for the s electrons, however, the exchange splitting of the d band and s - d scattering is taken into account. Therefore, the mean-free path of the conducting s electrons depends on the spin direction due to s - d scattering and the different d -electron density of states at the Fermi level, calculated by using the coherent potential approximation (CPA). A difficult but necessary task within the Kubo linear response formalism is to find the correct Green function (GF) matching at the interfaces. A review of some matching techniques can be found in Ref. 11. In our work we apply the variation-of-constant method¹² to construct a GF with continuous derivatives at the interfaces, enabling us to solve the differential equation

$$\left[\left(\frac{\partial^2}{\partial z^2} + (k_{Fn})^2 - \kappa^2 - E_n^{(0)} \right) \begin{pmatrix} 1 & 0 \\ 0 & 1 \end{pmatrix} - E_n^{(1)} \begin{pmatrix} \cos \gamma_n & \sin \gamma_n \\ \sin \gamma_n & -\cos \gamma_n \end{pmatrix} \right] \begin{bmatrix} G_n^{\uparrow\uparrow}(z, z') & G_n^{\uparrow\downarrow}(z, z') \\ G_n^{\downarrow\uparrow}(z, z') & G_n^{\downarrow\downarrow}(z, z') \end{bmatrix} = \frac{2Ma_0}{\hbar^2} \delta(z - z') \begin{pmatrix} 1 & 0 \\ 0 & 1 \end{pmatrix}. \quad (1)$$

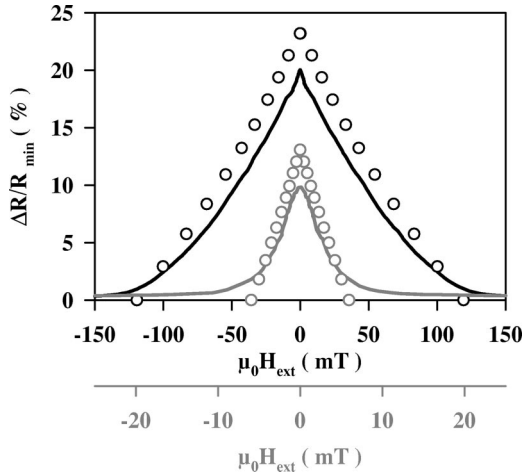


FIG. 1. Room temperature GMR vs field dependence of measured $\text{Py}_{1.8 \text{ nm}}//\{\text{Cu}_{0.9 \text{ nm}}/\text{Py}_{1.6 \text{ nm}}\}_{40}$ (black line) and $\text{Py}_{1.8 \text{ nm}}//\{\text{Cu}_{1.8 \text{ nm}}/\text{Py}_{1.6 \text{ nm}}\}_{40}$ (gray line) multilayers at the first and second antiferromagnetic coupling maximum, similar to Fig. 1 in Ref. 7. In comparison the corresponding quantum statistical calculations for $[\text{Py}_{1.6 \text{ nm}}/\text{Cu}_{0.9 \text{ nm}}]_3 \text{Py}_{1.6 \text{ nm}}$ (black circles) and for $[\text{Py}_{1.6 \text{ nm}}/\text{Cu}_{1.8 \text{ nm}}]_3 \text{Py}_{1.6 \text{ nm}}$ (gray circles) are shown. The transport parameters used are $\lambda_{\text{Py}}^{\uparrow} = 6.1 \text{ nm}$, $\lambda_{\text{Py}}^{\downarrow} = 0.9 \text{ nm}$, $\lambda_{\text{Cu}} = \lambda_{\text{Cu}}^{\uparrow} = \lambda_{\text{Cu}}^{\downarrow} = 33 \text{ nm}$, and $k_{\text{FPy}}^{\uparrow} = k_{\text{FPy}}^{\downarrow} = k_{\text{FCu}} = 0.1 \text{ nm}^{-1}$.

The angle γ_n between the magnetization of the n -th ferromagnetic layer and the quantization axis is provided by the numerical calculations (magnetization vectors are in the layer planes), k_{F_n} is the Fermi momentum in the n th layer, a_0 is the lattice constant, m the electron mass, and κ the in-plane momentum. The corresponding energies can be written as

$$E_n^{(0)} = \frac{1}{2}(\Sigma^{\uparrow} + \Sigma^{\downarrow}), \quad E_n^{(1)} = \frac{1}{2}(\Sigma^{\uparrow} - \Sigma^{\downarrow}), \quad (2)$$

where the exchange splitting of the s electrons with spin σ is determined by the real part of the electron self-energy Σ^{σ} , and their inverse lifetime is proportional to the imaginary part. Whereas $E_n^{(1)} \neq 0$ for all ferromagnetic layers, $E_n^{(1)} = 0$ for the Cu spacers. Details concerning the solution of Eq (1) are presented elsewhere¹³.

A direct comparison of measured and calculated GMR characteristics at room temperature of the two underlying base systems $\{\text{Cu}_{0.9 \text{ nm}}/\text{Py}_{1.6 \text{ nm}}\}_N$ at the first and $\{\text{Cu}_{1.8 \text{ nm}}/\text{Py}_{1.6 \text{ nm}}\}_N$ at the second afcm is given in Fig. 1. The absolute difference between calculated and measured GMR amplitudes is 3.2 and 3.3 %, respectively, whereas the saturation fields are in good agreement. The latter feature is a consequence of using the numerically obtained γ_n as input quantities. To achieve this good match between measured and calculated GMR characteristics the spin-dependent mean-free paths for the spin-up and spin-down electrons in Py were assumed to be $\lambda_{\text{Py}}^{\uparrow} = 6.1 \text{ nm}$ and $\lambda_{\text{Py}}^{\downarrow} = 0.9 \text{ nm}$, respectively, and the mean-free path in Cu was $\lambda = 33 \text{ nm}$. These values are 33, 50, and 46 %, respectively, larger than those determined by Gurney *et al.*¹⁴ for spin valve structures using the classical solution of the Boltzmann transport equa-

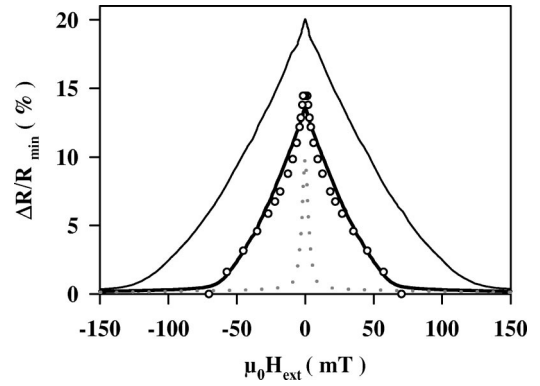


FIG. 2. Measured room temperature GMR vs field dependence of $\text{Py}_{1.8 \text{ nm}}//\{\text{Cu}_{1.8 \text{ nm}}/\text{Py}_{1.6 \text{ nm}}\}_1/[\text{Cu}_{0.9 \text{ nm}}/\text{Py}_{1.6 \text{ nm}}]_1\}_{20}$ (black line), together with the one of the underlying base systems $\text{Py}_{1.8 \text{ nm}}//\{\text{Cu}_{0.9 \text{ nm}}/\text{Py}_{1.6 \text{ nm}}\}_{40}$ (gray line) and $\text{Py}_{1.8 \text{ nm}}//\{\text{Cu}_{1.8 \text{ nm}}/\text{Py}_{1.6 \text{ nm}}\}_{40}$ (gray dotted line) multilayers at the first and second antiferromagnetic coupling maximum, similar to Fig. 1 in Ref. 7. In comparison the corresponding quantum statistical calculations for $[\text{Py}_{1.6 \text{ nm}}/\text{Cu}_{1.8 \text{ nm}}]_1[\text{Py}_{1.6 \text{ nm}}/\text{Cu}_{0.9 \text{ nm}}]_1\text{Py}_{1.6 \text{ nm}}$ (black circles) are shown. The transport parameters used are $\lambda_{\text{Py}}^{\uparrow} = 6.1 \text{ nm}$, $\lambda_{\text{Py}}^{\downarrow} = 0.9 \text{ nm}$, $\lambda_{\text{Cu}} = \lambda_{\text{Cu}}^{\uparrow} = \lambda_{\text{Cu}}^{\downarrow} = 33 \text{ nm}$ and $k_{\text{FPy}}^{\uparrow} = k_{\text{FPy}}^{\downarrow} = k_{\text{FCu}} = 0.1 \text{ nm}^{-1}$.

or, or extracted from measured resistivities by using the free electron model. This difference may reflect a smaller degree of shunting in our multilayers due to the special spin valve structure in Ref. 14, and a less diffusive scattering due to smoother interfaces. The Fermi vectors used for spin-up and spin-down electrons in Py as well as for the electrons in Cu were set to $k_F = 0.1 \text{ nm}^{-1}$ each. This is very close to the value of $k_F^{\text{RKKY}} = 0.116 \text{ nm}^{-1}$ of the electrons responsible for the RKKY interaction in these multilayers, estimated from the aliasing effect as described by the relation¹⁵

$$\Lambda = \left| \frac{1}{\left(\frac{\pi}{k_F^{\text{RKKY}}} \right) - \frac{n}{d_{111}^{\text{Cu}}} \right|^{-1} \quad (3)$$

with $n = 1$, taking into account the measured GMR oscillation wavelength of $\Lambda = 0.9 \text{ nm}$ (Ref. 16) and assuming a dominant [111] growth direction. These transport parameters were also used to calculate the GMR characteristics of CML structures as discussed below.

Figure 2 confirms that the measured GMR vs field curve for $N = 1$ (see Fig. 1) is basically the average of the two base systems at the first and second AFCM. The corresponding bilinear coupling constants J_L were determined from the experimental curves by means of Eq. (4) (see Ref. 16) which relates J_L to the thickness t_{Py} of the Py layer, their saturation magnetization M_{Py} and the saturation field

$$H_{\text{saturation}}^{\text{experiment}} = \frac{4J_L}{M_{\text{Py}}t_{\text{Py}}}. \quad (4)$$

Table I shows that indeed $J_L(N = 1) = 0.5[J_L(t_{\text{Cu}} = 0.9 \text{ nm}) + J_L(t_{\text{Cu}} = 1.8 \text{ nm})]$. This behavior can easily be understood by implying a dominating nearest-neighbor interaction in

TABLE I. Comparison of calculated and measured coupling strengths J_L .

Structure	Experimental	Calculated
$\text{Py}_{1.8 \text{ nm}} // \{ \text{Cu}_{0.9 \text{ nm}} / \text{Py}_{1.6 \text{ nm}} \}_{40}$	0.021 mJ/m ²	1.76 mJ/m ²
$\text{Py}_{1.8 \text{ nm}} // \{ \text{Cu}_{1.8 \text{ nm}} / \text{Py}_{1.6 \text{ nm}} \}_{40}$	1.51×10^{-3} mJ/m ²	0.31 mJ/m ²
$\text{Py}_{1.8 \text{ nm}} // \{ [\text{Cu}_{1.8 \text{ nm}} / \text{Py}_{1.6 \text{ nm}}]_1 / [\text{Cu}_{0.9 \text{ nm}} / \text{Py}_{1.6 \text{ nm}}]_1 \}_{20}$	0.071 mJ/m ²	1.03 mJ/m ²

this CML structure, in which every Py layer is strongly coupled to the nearest ferromagnetic layers but weakly coupled to the next-nearest layers. Thus, the resulting effective coupling constant is the average of the two. To prove this assumption, we have performed *ab initio* electronic structure calculations to determine the behavior of J_L in $\text{Py}_{1.8 \text{ nm}} // [[\text{Cu}_{1.8 \text{ nm}} / \text{Py}_{1.6 \text{ nm}}]_1 [\text{Cu}_{0.9 \text{ nm}} / \text{Py}_{1.6 \text{ nm}}]_1]_{20}$ (structure C), $\text{Py}_{1.8 \text{ nm}} // \{ \text{Cu}_{0.9 \text{ nm}} / \text{Py}_{1.6 \text{ nm}} \}_{40}$ (structure A) and $\text{Py}_{1.8 \text{ nm}} // \{ \text{Cu}_{1.8 \text{ nm}} / \text{Py}_{1.6 \text{ nm}} \}_{40}$ (structure B). To avoid the numerical effort of a CPA calculation for disordered Py, we considered Co/Cu multilayers instead, but used identical structure parameters regarding stacking sequence, layer thickness, and number of repeats as in the experimentally realized {Py/Cu} multilayers. The large number of atoms in the supercell required a recently developed linear-scaling electronic structure calculation scheme (screened-Korringa-Kohn-Rostoker method^{17,18}). The coupling phenomenon in the structures A, B, and C has been treated by comparing the total energies $E_{N,\alpha}$ of their magnetic configurations with all magnetic moments in parallel or antiparallel. We focussed on the nearest-neighbor coupling between adjacent magnetic layers and used a Heisenberg model to calculate E_N for the two magnetic configurations from which the J_L can then be extracted:

$$E_N = \sum_{i,j}^{t=|\vec{R}_i - \vec{R}_j|} J_L(t) M_i M_j. \quad (5)$$

These values are listed in Table I. Although the absolute values are two orders of magnitude larger than the experimentally determined ones, they confirm the relationship $J_L(C) = 0.5[J_L(A) + J_L(B)]$. The much larger calculated absolute values of the coupling constants may be due to our treatment of {Co/Cu}—instead of {Py/Cu} multilayers and by chemical disorder or roughness at the interfaces^{19,20} which can significantly lower the coupling strength. The result of our quantum statistical calculation is displayed in Fig. 2. The difference between the experimental and the calculated GMR amplitude is only about 1%, and the field dependencies are in excellent agreement. The fact that a minimum layer sequence of $[\text{Py}_{1.6 \text{ nm}} / \text{Cu}_{1.8 \text{ nm}}]_1 [\text{Py}_{1.6 \text{ nm}} / \text{Cu}_{0.9 \text{ nm}}]_1 \text{Py}_{1.6 \text{ nm}}$ is sufficient in these calculations to match the GMR characteristics of the whole $\text{Py}_{1.8 \text{ nm}} // [[\text{Cu}_{1.8 \text{ nm}} / \text{Py}_{1.6 \text{ nm}}]_1 / [\text{Cu}_{0.9 \text{ nm}} / \text{Py}_{1.6 \text{ nm}}]_1]_{20}$ multilayer stack can again be taken as an indication of the dominating nearest-neighbor coupling. From simple geometrical considerations the CML characteristics for $N \geq 2$ should reflect the three contributions from the structures A and B and the mixed case C, scaled with $(N-1)/2N$ for A and B and $1/N$ for C. Hence, the latter

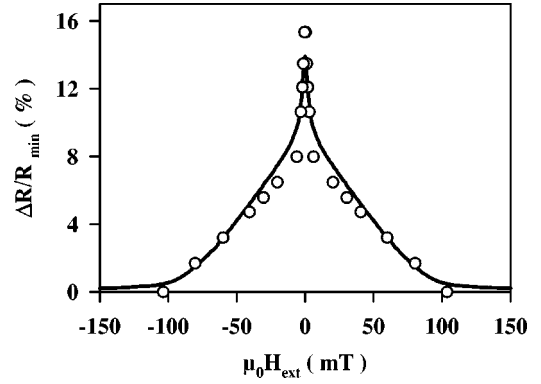


FIG. 3. Measured room temperature GMR characteristics of $\text{Py}_{1.8 \text{ nm}} // [[\text{Cu}_{1.8 \text{ nm}} / \text{Py}_{1.6 \text{ nm}}]_2 / [\text{Cu}_{0.9 \text{ nm}} / \text{Py}_{1.6 \text{ nm}}]_2]_{10}$ (black line) similar to Fig. 2(a) in Ref. 7, and for comparison the corresponding quantum statistical calculations for $[\text{Py}_{1.6 \text{ nm}} / \text{Cu}_{1.8 \text{ nm}}]_2 [\text{Py}_{1.6 \text{ nm}} / \text{Cu}_{0.9 \text{ nm}}]_2 \text{Py}_{1.6 \text{ nm}}$ (black circles). The transport parameters used are $\lambda_{\text{Py}}^\uparrow = 6.1 \text{ nm}$, $\lambda_{\text{Py}}^\downarrow = 0.9 \text{ nm}$, $\lambda_{\text{Cu}} = \lambda_{\text{Cu}}^\uparrow = \lambda_{\text{Cu}}^\downarrow = 33 \text{ nm}$, and $k_{\text{FPy}}^\uparrow = k_{\text{FPy}}^\downarrow = k_{\text{FCu}} = 0.1 \text{ nm}^{-1}$.

should vanish with increasing N . Therefore, CML with large N can be understood as a well separated two-block system consisting of $[\text{Py}_{1.6 \text{ nm}} / \text{Cu}_{1.8 \text{ nm}}]_N // [\text{Py}_{1.6 \text{ nm}} / \text{Cu}_{0.9 \text{ nm}}]_N$. For comparison the experimentally obtained GMR characteristics of the CML with $N=2$ is shown in Fig. 3. As can be seen clearly, there is no indication of three contributions. Instead, the saturation fields of the structures A and B can be identified at 103.8 and 5.9 mT, respectively. The lack of a visible C contribution can be understood with the help of the numerically calculated magnetization angles: It turns out, that the magnetization C is either not switching at all or it is switching together with the magnetization of the neighboring layers; hence it is not detected. The quantum statistical calculation is again in good agreement with the experimental curve.

In summary, it has been shown that a quantum statistical treatment, together with the numerically determined orientation of magnetic moments, is a very powerful tool to reliably predict the GMR characteristics even of complex multilayered structures. *Ab initio* electronic structure calculations confirmed that the interplay of adjacent but different antiferromagnetic exchange couplings in these CML is physically based on a dominant nearest-neighbor interaction. The good agreement of experimental and calculated GMR characteristics suggests to use this combined approach (i) to “measure” spin-dependent transport properties such as mean-free paths and Fermi vectors and (ii) to employ it to reliably design and predict GMR characteristics for specific applications.

ACKNOWLEDGMENTS

The work has been supported by the Deutsche Forschungsgemeinschaft in the “Forschergruppe Nanometer-Schichtsysteme.” A. V. Vedyayev acknowledges the CENG DRMC SP2M and Bielefeld University for hospitality and the Russian Foundation of Fundamental Research for financial support. M. Ye. Zhuravlev is grateful to Bielefeld University for hospitality.

- *On leave from Institute of General and Inorganic Chemistry, RAS, Leninskii prosp., 31, Moscow 117907, Russian Federation.
- †On leave from Physical Department of Moscow State University, Moscow 119899, Russian Federation.
- ¹Special issue of *J. Magn. Magn. Mater.* **200**, No. 1-3 (1999).
- ²B.Yu. Yavorsky, I. Mertig, A.Ya. Perlov, A.N. Yaresko, and V.N. Antonov, *Phys. Rev. B* **62**, 9586 (2000).
- ³P.M. Levy, S. Zhang, and A. Fert, *Phys. Rev. Lett.* **65**, 1643 (1990).
- ⁴A. Vedyayev, B. Dieny, and N. Ryzhanova, *Europhys. Lett.* **19**, 329 (1992); A. Vedyayev, C. Cowache, N. Ryzhanova, and B. Dieny, *J. Phys.: Condens. Matter* **5**, 8289 (1993).
- ⁵H.E. Camblong, P.M. Levy, and S. Zhang, *Phys. Rev. B* **51**, 16 052 (1995).
- ⁶M.Ye. Zhuravlev, H.O. Lutz, and A.V. Vedyayev, *Phys. Rev. B* **63**, 174409 (2001)
- ⁷S. Heitmann, A. Hütten, T. Hempel, W. Schepper, and G. Reiss, *J. Appl. Phys.* **87**, 4849 (2000).
- ⁸S. Heitmann, A. Hütten, T. Hempel, W. Schepper, and G. Reiss, *J. Magn. Magn. Mater* **226-230**, 1752 (2001).
- ⁹W. Schepper, A. Hütten, and G. Reiss, *J. Appl. Phys.* **88**, 993 (2000)
- ¹⁰A. Vedyayev, B. Dieny, N. Ryzhanova, J.B. Genin, and C. Cowache, *Europhys. Lett.* **25**, 465 (1994); A. Vedyayev, N. Ryzhanova, B. Dieny, P. Dauguet, P. Gandit, and J. Chaussy, *Phys. Rev. B* **55**, 3728 (1997).
- ¹¹R. Perez-Alvarez, F. Garcia-Moliner, and V.R. Velasco, *J. Phys.: Condens. Matter* **7**, 2037 (1995).
- ¹²E.A. Coddington and N. Levinson, *Theory of Ordinary Differential Equations* (McGraw-Hill, New York, 1955).
- ¹³M.Ye. Zhuravlev, H.O. Lutz, and A.V. Vedyayev, *J. Phys. A* **34**, 8383 (2001).
- ¹⁴B.A. Gurney, V.S. Speriosu, J.-P. Nozieres, H. Lefakis, D.R. Wilhoit, and O.U. Need, *Phys. Rev. Lett.* **71**, 4023 (1993).
- ¹⁵R. Coehoorn, *Phys. Rev. B* **44**, 9331 (1991).
- ¹⁶A. Hütten, S. Mrozek, S. Heitmann, T. Hempel, H. Brückl, and G. Reiss, *Acta Mater.* **47**, 4245 (1999)
- ¹⁷R. Zeller, P.H. Dederichs, B. Újfalussy, L. Szunyogh, and P. Weinberger, *Phys. Rev. B* **52**, 8807 (1995).
- ¹⁸P. Zahn, I. Mertig, R. Zeller, and P.H. Dederichs, in *Magnetic Ultrathin Films, Multilayers and Surfaces—1997*, edited by J. Jobin, D. Kubinski, K. Barmak, P. Dederichs, W. de Jong, T. Katayama, and A. Schuhl, MRS Symposia Proceedings No. 475 (Materials Research Society, Pittsburgh, 1997), p. 525.
- ¹⁹P. Lang, L. Nordström, K. Wildberger, R. Zeller, P.H. Dederichs, and T. Hoshino, *Phys. Rev. B* **53**, 9092 (1996).
- ²⁰J. Mathon, M. Villeret, A. Umerski, R.B. Muniz, J. d'Albuquerque e Castro, and D.M. Edwards, *Phys. Rev. B* **56**, 11 797 (1997).